Synthesis and characterization of solid polymethylaluminoxane "sMAO"; a bifunctional activator and support for slurry-phase ethylene polymerization

Alexander F. R. Kilpatrick,[†] Jean-Charles Buffet,[†] Peter Nørby,[†] Nicholas H. Rees,[†] Nicholas P. Funnell,[‡] Saovalak Sripothongnak,[§] and Dermot O'Hare[†]*

[†]Chemistry Research Laboratory, Department of Chemistry, University of Oxford, 12 Mansfield Road, Oxford, OX1 3TA, U.K.

[‡]ISIS Neutron and Muon Facility, Rutherford Appleton Laboratory, Chilton, OX11 0QX, U.K.

[§]SCG Chemicals Co., Ltd, 1 Siam Cement Rd, Bangkok 10800, Thailand.

Supporting Information Placeholder

ABSTRACT: An insoluble form of methylaluminoxane, also known as solid polymethylaluminoxane (sMAO), has been synthesized by the controlled hydrolysis of trimethylaluminum (TMA) with benzoic acid, followed by thermolysis. Characterization of sMAO by multinuclear NMR spectroscopy in solution and the solid state reveals an aluminoxane structure that features "free" and bound TMA and incorporation of a benzoate residue. Total X-ray scattering (or pair distribution function, PDF) measurements on sMAO allow comparisons to be made with simulated data for DFT modeled structures of MAO. Several TMA-bound $(AlOMe)_n$ cage and nanotubular structures with n>10 are consistent with the experimental data. The measured Brunauer–Emmett–Teller (BET) surface area of sMAO ranges between 312 – 606 m^2 g^{-1} and shows an N_2 adsorption/desorption isotherm consistent with a non-porous material. sMAO can be utilized to support metallocene pre-catalysts in slurry-phase ethylene polymerization reactions. Metallocene pre-catalyst *rac*-ethylenebis(1-indenyl)-dichlorozirconium, *rac*-(EBI)$ZrCl_2$ was immobilized on sMAO samples, to afford solids which showed very high polymerization activities in hexane, comparable to those of the respective homogeneous catalysts formed by treatment of the pre-catalysts with MAO. *rac*-(EBI)$ZrCl_2$ immobilized on an sMAO containing an Al:O ratio of 1.2 gave the highest ethylene polymerization activity.

INTRODUCTION

Methylaluminoxane (MAO) is the most commonly used activator for metallocenes in olefin polymerization reactions.[1] Despite its widespread use, there remains considerable debate about the precise composition, structure and catalytic function of MAO.[2-5] Fundamental investigations have yielded important insights into the general properties,[6-12] but precise details still remain uncertain.

MAO is routinely synthesized by the partial hydrolysis of trimethylaluminum (TMA) using water or a metal hydrate salt, but these reactions are highly exothermic and are difficult to control. To circumvent these problems non-hydrolytic routes to MAO have been developed, for example by reaction of TMA with a carbonyl-containing compound such as CO_2, $MeCO_2H$ or Ph_2CO.[13] The less reactive nature of the C–O bond compared with the O–H bond allows milder non-hydrolytic syntheses to be carried out in a much more controlled manner.

In 1974, Mole and co-workers reported the thermolysis of TMA with aromatic acids, with the aim of preparing C-methylated organic derivatives (Scheme 1).[14]

Scheme 1. C-methylation product of carboxylic acids by TMA according to ref 14**.**

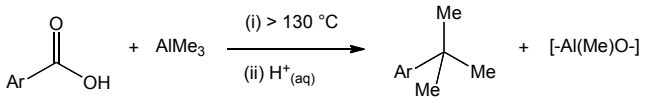

Cramail and co-workers subsequently studied the reactions of carboxylic acids and TMA in-depth, as a route to MAO-type derivatives as activators for metallocene and post-metallocene complexes in olefin polymerization.[15-18] These researchers found that the main products formed depend on the temperature and on the initial TMA/benzoic acid ratio. At room temperature with a 1:1 ratio an Al-carboxy species (**I**) is formed (Scheme 2). As the TMA:benzoic acid ratio is increased from 1 to 3 mixtures of **I** and an Al-alkoxy species $PhCMe_2OAlMe_2$ (**II**) together with monomeric and/or oligomeric aluminoxanes with speculative structure "Me_2Al-O-$AlMe_2$" were formed. In the room temperature reaction with a

TMA:benzoic acid ratio of 3, Al-alkoxide (**II**) and these aluminoxane species were obtained as a homogeneous mixture. The latter mixture proved to be an efficient activator for the post-metallocene pre-catalyst [2,6-bis[1-((2,6-diisopropylphenyl)imino)ethyl)-pyridine]iron dichloride in ethylene polymerization. A UV-Vis spectroscopic study showed that only the "Me_2Al-O-$AlMe_2$" aluminoxane components of this mixture could activate the metallocene pre-catalyst (EBI)$ZrCl_2$.[17]

Scheme 2. Reaction steps between benzoic acid and TMA at 20 °C according to ref 17.

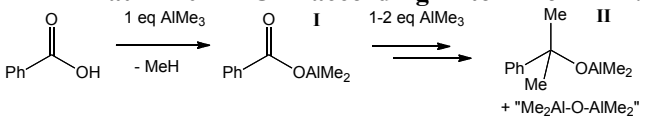

Cramail and co-workers noted that above 60 °C and a TMA:benzoic acid ratio of 3 led to the precipitation of higher aluminoxane (MAO-like) oligomers *via* a condensation reaction (Scheme 3).

Scheme 3. Condensation reaction of "$Me_2AlOAl(Me)OAlMe_2$" according to ref 17.

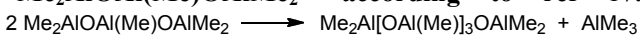

These insoluble aluminoxane oligomers, also known as solid polymethylaluminoxanes (sMAO) have been reported by Kaji *et al.* in the patent literature as an effective support for metallocene pre-catalysts in slurry-phase olefin polymerization.[19]

A recent report from our own laboratory described sMAO as an effective support for a tungsten imido complex, W(NDipp)Me_3Cl (Dipp = 2,6-^{i}Pr-C_6H_3). This sMAO immobilized complex shows higher activity for the selective dimerization of ethylene to yield 1-butene compared to an analogous homogeneous system using soluble MAO.[20] We are now extending this work to the development of well-defined, immobilized group 4 metallocene complexes for slurry phase ethylene polymerization,[21-26] The overall aims are to reduce the cost of the final solid catalyst whilst maintaining catalyst productivity and performance levels.

Although MAO derivatives produce highly active metallocene-based catalytic systems, the use of MAO in large excess is still currently an important limitation for the development of metallocenes at the industrial scale. Current estimates indicate that the price of the MAO co-catalyst contributes to *ca.* 90% of the final catalyst system.

Herein we report our investigations on the synthesis and characterization of solid forms of MAO (sMAO), which are emerging as a highly promising mulifunctional support material for producing high performance immobilized "single-site" catalysts in slurry-phase olefin polymerization reactions.[27]

RESULTS AND DISCUSSION

Synthesis of sMAO. The synthesis of sMAO was adapted from the procedure described by Kaji *et al.* in the patent literature (Scheme 4).[19] We found that the nature of the sMAO formed was very sensitive to the Al:O ratio and the time and temperature of the 2 separate thermolysis steps. For brevity, each sMAO prepared herein will be represented as sMAO(Al:O ratio/Step 2 temperature in °C, time in h/Step 3 temperature in °C, time in h). Hence, the synthesis conditions outlined in Scheme 4 would yield sMAO(1.2/80,28/100,14).

Scheme 4. Synthesis of sMAO-(1.2/80,28/100,14).

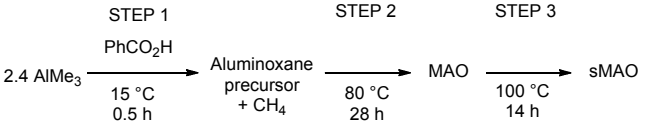

Following the thermolysis steps the reaction mixture was cooled to room temperature, addition of hexane resulted in the precipitation of a white solid which was isolated by filtration, washed with hexane and dried *in vacuo*, (84% yield based on 41.3 wt% Al).

Characterization of sMAO. The synthesized sMAO was sparingly soluble in THF-d_8, allowing for its characterization by solution NMR spectroscopy. The ^{1}H NMR spectrum shows a resonance between 0.03 and –1.57 ppm, assigned to the methyl protons of the sMAO, which is broad due to the oligomeric nature of the material (Figure 1). Within this broad feature is superimposed a sharp resonance at –0.60 ppm, which is assigned to the methyl protons of TMA included within the sMAO structure. The sharp signal at –0.96 ppm is assigned to 'free' TMA, which is an inherent part of all MAO compositions.[28] The amount of free TMA was determined by peak fitting and integration of the ^{1}H spectra in the methyl region (0 to –1.5 ppm) and expressed in terms of mol% of TMA CH_3 groups with respect to MAO CH_3 groups. This analysis of sample sMAO(1.2/80,28/100,14) resulted in a value of 13.8 mol% TMA (Table S1).

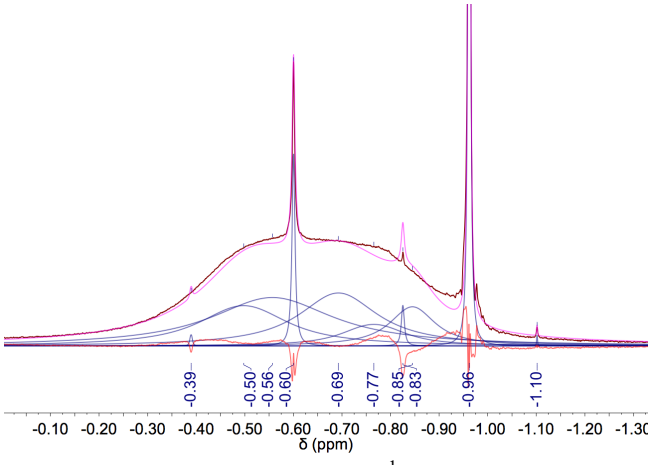

Figure 1. Methyl region of the ^{1}H NMR spectrum of sMAO(1.2/80,28/100,14) in THF-d_8. Dark red is the experimental spectrum, blue lines are the fitted peaks,

pink line is the sum of the fitted peaks, red line is the residual.

On close inspection of the ^{1}H NMR spectrum, three broad resonances are observed between 8.25 – 7.60 ppm (Figure S1), assigned to the aromatic protons of benzoate residues in the structure. It is postulated that the aromatic rings of benzoic acid can have a template effect in the self-association reaction of lower-aluminoxanes to form sMAO. This was verified via an independent synthesis of an isotopically labeled α^{13}C-sMAO(1.2/80,28/100,14) sample using α-^{13}C labelled benzoic acid. The ^{13}C{^{1}H} NMR spectrum shows a broad signal at 176.1 ppm assigned to the labelled carbonyl carbon (Figure S2), indicating that this functional group remains in the solid isolated after thermolysis and work-up. The solid state ^{13}C CP-MAS NMR spectrum at 10 kHz showed an intense resonance at 177.4 ppm in the labelled sample (Figure 2b); the corresponding signal (in relatively low intensity) was identified at 117.2 ppm in an unlabeled sample. Integration of the ^{13}C CP-MAS spectra reveals a ca. 0.9% incorporation of benzoate groups relative to CH_3 groups in α^{13}C-sMAO(1.2/80,28/100,14).

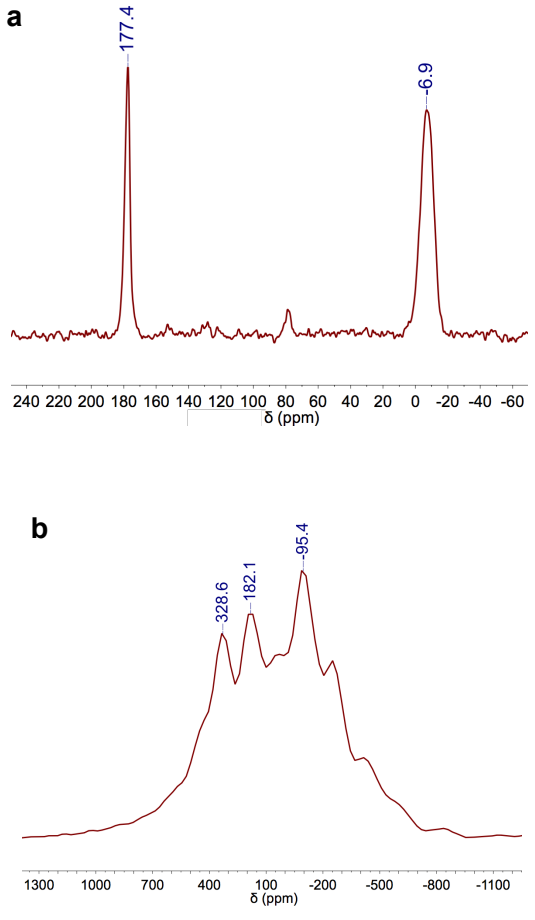

Figure 2. (a) ^{13}C CP-MAS and (b) ^{27}Al DP-MAS SSNMR spectra of α^{13}C-sMAO(1.2/80,28/100,14).

The ^{27}Al{^{1}H} NMR spectrum in THF-d_8 solution (Figure S3) shows a background signal centered at 67.6 ppm, and a relatively low intensity resonance at 189.1 ppm assigned to the Al environment in sMAO or TMA bound within the structure. For comparison, the ^{27}Al{^{1}H} NMR spectrum of pure TMA in THF-d_8 consists of a single signal at 183.5 ppm. Experimental and computational ^{27}Al SSNMR spectroscopic studies of dried MAO, polymeric MAO-diol adducts and discrete aluminum clusters have been reported previously.[29-31] The ^{27}Al DP-MAS SSNMR spectrum of sMAO at 15 kHz shows a broad envelope, as expected for a quadropolar (I = 5/2) nucleus, between 630 – –715 ppm (Figure 2b). This spectrum is comparable to that of the planar, 3-coordinate (aminato)trialuminum ring, [(MeAl)(N(DIP))]$_3$, reported by Bryant *et al.*, which was simulated using the sum of two ^{27}Al powder patterns.[29] Hence, we postulate at least two major ^{27}Al components are present in sMAO.

A sample of sMAO(1.2/80,28/100,14) was sealed in a glass capillary and was subject to total X-ray scattering measurements using a Ag-source PANalytical Empyrean, resulting in a useable Q-range from 0.4–16.5 Å^{-1}. The pair distribution function (PDF) was obtained by subtracting scattering from the sample container and Fourier transforming the corrected total X-ray scattering data in GudrunX.[32] The PDF data were compared with calculated PDFs, using PDFgui,[33] of MAO structures proposed on the basis of DFT calculations.[7,34-36] These include spherical MAO cages (with the formula (AlOMe)$_{n,c}$, n = 6−20) and free TMA, as well as finite (2,2) MAO nanotubes that have been capped at the ends with TMA (with the formula (AlOMe)$_{n,t}$·(AlMe$_3$)$_m$, n = 6−20 and even, m = 1−4). Note, the subscripts 't' and 'c' used in the nomenclature outlined by Falls *et al.* denote the tubular and cage structures respectively.[36] Figures S5 and S6 show a comparison of the experimental and calculated PDF data. The difference between the underlying forms of the data and the calculated PDFs is described in the S.I. Several different calculated structures are consistent with the PDF data. However, given that sMAO contains free TMA, the structures that come closest to accounting for the experimental data were those of nanotubular MAO (AlOMe)$_{9,t}$·(AlMe$_3$)$_3$ (Figure 3a) reported by Linnolahti *et al.*,[7] and spherical MAO cages (AlOMe)$_{20,c}$,·(AlMe$_3$)$_m$, m = 1,2 (Figure 3b) reported by Falls *et al.*[36] Smaller cage structures, (AlOMe)$_{n,c}$ where n<10, are missing the long range intra-atomic distances seen in the PDF suggesting these are not major components of sMAO.

Comparison of the measured PDF data with those calculated for (AlOMe)$_{9,t}$·(AlMe$_3$)$_3$, as a plausible model structure, shows that the local structure is broadly similar up to ca. 4.5 Å, above which atom-atom correlations diminish rapidly as a function of distance (Figure 4). Figure S7 shows a simulation of the nanotube model with PDFgui variables (including particle diameter and

atomic displacement parameters) fitted to the experimental data. It is unlikely that the complexity of the sample structure can be captured fully by the models here, given the uncertainty in sample composition, density, and thermal vibrations that are not accounted for in the calculated PDFs.

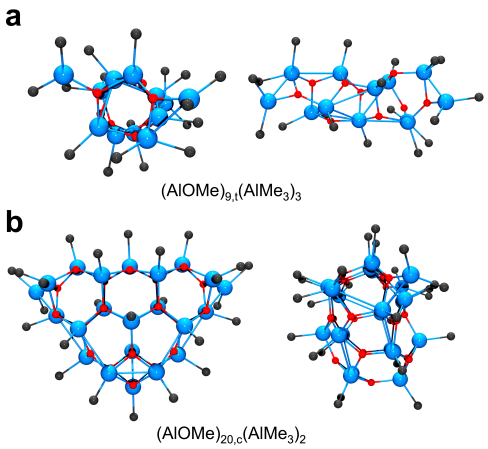

Figure 3. 'End-on' and 'side-on' views of the DFT optimized structures of (a) $(AlOMe)_{9,t}\cdot(AlMe_3)_3$ and (b) $(AlOMe)_{20,c}\cdot(AlMe_3)_2$, reproduced from published coordinates.[7,36] Al/O/C atoms colored in blue/red/grey respectively. H atoms removed for clarity.

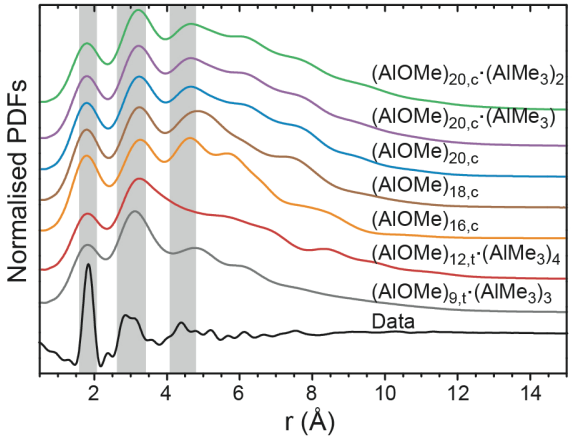

Figure 4. Stack plot showing X-ray PDF ($D(r)$) of measured data (black line) and DFT optimized structures of MAO calculated with pdfGUI (colored lines).[7,36]

Looking at the partial PDFs in Figure 5, it can be seen that the first, most intense peak at ca. 2.0 Å arises from Al–O and Al–C correlations, which make up the backbone of MAO. The second significant peak at ca. 3.5 Å is comprized of contributions from several atom-atom correlations, notably Al–Al, although there is a peak splitting in the data not predicted by the DFT models. This may indicate the possibility of two different sets of Al–Al correlations in the as-synthesized sMAO sample.

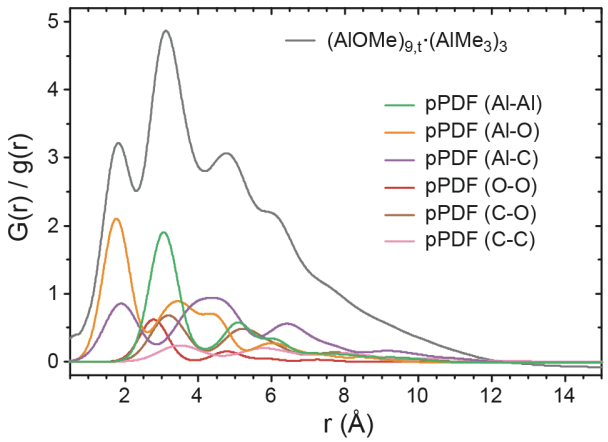

Figure 5. Partial PDFs (pPDF, $g(r)$) of the disordered $(AlOMe)_{9,t}\cdot(AlMe_3)_3$ model,[7] showing the different contributions the peaks in the PDF.

Figure 6 shows an SEM image of a sMAO sample revealing a 'popcorn' morphology with particle sizes ranging from 5-8 µm. The particle size distribution of sMAO(1.2/80,28/100,14) dispersed in hexane was evaluated via laser diffraction method, which revealed a median particle diameter $D(0.5)$ of 19.8 µm (Figure S8).

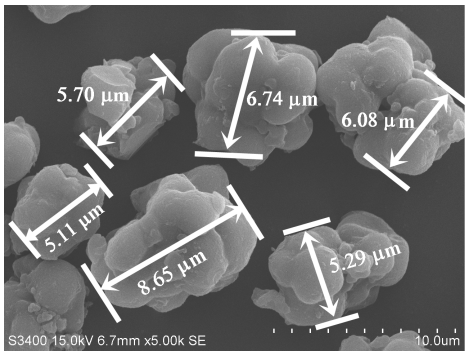

Figure 6. SEM image of sMAO sample.

The specific surface area and porosity of the sMAO samples were determined by N_2 physisorption using Brunauer–Emmett–Teller (BET) theory. The BET surface area for sMAO(1.2/80,28/100,14) is 589.1 m^2g^{-1}, which is over an order of magnitude higher than those reported for particulate MAO-diol adducts (20.3 – 34.6 m^2 g^{-1}).[30] The data obtained (Figure 7) are consistent with a Type II isotherm (according to the 2015 IUPAC recommendations),[37] which is typically given by inert gas physisorption on nonporous or macroporous adsorbents.

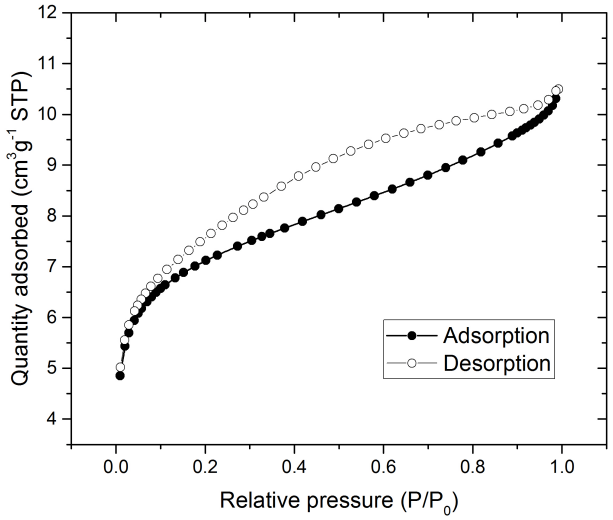

Figure 7. BET measurements of sMAO sample.

Ethylene polymerization studies

The complex *rac*-ethylenebis(1-indenyl) zirconium dichloride, *rac*-(EBI)$ZrCl_2$, was chosen as a control pre-catalyst for these studies, given its robust structure and high activity for the polymerization of ethylene. Immobilization of the complex was achieved by addition of toluene to a mixture of *rac*-(EBI)$ZrCl_2$ and the sMAO support (200:1 Al:Zr mol ratio), followed by heating at 80 °C for two hours. After work-up, bright orange powders were isolated in good yield (>80%). The ethylene polymerization activity observed for *rac*-(EBI)$ZrCl_2$ on sMAO (1.2/80,28/100,14) was 13066 $kg_{PE}mol_{Zr}^{-1}h^{-1}$ which is significantly higher than the activity we have recently reported for this complex supported on MAO modified MgAl-SO_4 layered double hydroxides (1841 $kg_{PE}mol_{Zr}^{-1}h^{-1}$),[21] and with other MAO-based supports under similar polymerization conditions.[21,22,24] Figure S9 shows the SEM images of the polyethylene samples obtained.

Synthetic optimization of sMAO. The effect of various parameters in the synthetic procedures (Al:O ratio, reagent amounts, heating temperature and time period) was systematically studied with a view to identifying trends in TMA content, surface area and their link with polymerization activity. The metric for selecting the best conditions was to deliver the optimum polymerization activity per mole of catalyst. In the proposed reaction sequence at room temperature (Scheme 2),[15,17] step 1 involves an initial protonolysis of benzoic acid by TMA to form methane gas and a toluene-soluble Al-carboxy species **I**. Therefore the stoichiometric ratio of initial reactants is likely to be an important factor in this step, and may have an effect on the amount of 'free' TMA present in sMAO ultimately produced.

Step 1: Al:O Ratio

Varying amounts of benzoic acid (BA) were added to a fixed amount of TMA in toluene. The temperature and time period for thermolysis were then controlled to step 2: 80 °C, 28 h, and step 3: 100 °C, 14 h, as represented by the short-hand description sMAO(Al:O/80,28/100,14). Characterizing data are collected in Table 1, showing there is no apparent correlation between the Al:O ratio of initial reagents and free TMA content determined by ^{1}H NMR spectroscopy in the sMAO samples. However, these data should be treated with caution given that solution NMR spectra only provide information on the components of the sMAO sample which are soluble in THF-d_8.

Table 1. Effect of Al:O ratio on sMAO-(Al:O/80,28/100,14). Data in parentheses are for repeat samples.

Al:O	TMA (mol%)	Yield (%)	Al (wt%)	BET[a]	Activity[b]
1.0	1.0	26	40.4	440.7	*
1.1	20.8	93	43.6	605.5	5783
1.2	13.8	82	41.3	589.1	13066
1.3	7.5 (6.8)	53 (56)	37.9	386.2	4289
1.4	11.0	42	43.0	366.7	6192
1.6	11.6	58	38.4	312.3	4220

**rac*-(EBI)$ZrCl_2$ did not immobilize after 2 h at 80 °C in toluene; [a]m^2 g^{-1} [b]All ethylene polymerization experiments were conducted at least twice to ensure the reproducibility of the corresponding outcome. Mean activities are quoted in units of $kg_{PE}mol_{Zr}^{-1}$ h^{-1}

The polymerization data show that there is no clear trend between Al:O ratio and activity for *rac*-(EBI)$ZrCl_2$ on sMAO (Figure 8), the most active ratio is 1.2. In a series control experiments the Al:O ratio was varied by keeping BA amount constant and varying TMA, and the polymerization activity data show the same general trend (Figure S10).

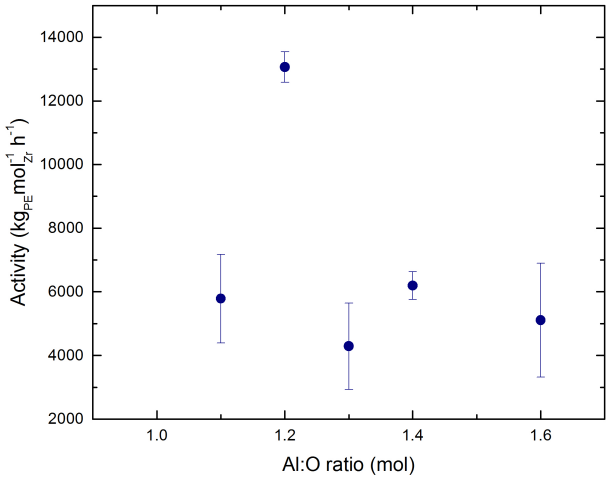

Figure 8. Effect of Al:O initial ratio on polymerization activity for *rac*-(EBI)$ZrCl_2$ on sMAO(Al:O/80,28/100,14). Data are an average of at least 2 runs with ±1 SD error.

Comparison of Al:O ratio and BET surface area (Figure S11) reveals a general decrease in surface area in the Al:O range 1.1 – 1.6, which may explain why the activation efficiency of *rac*-(EBI)$ZrCl_2$ decreases for higher Al:O ratios. However, the data for the sample synthesized with Al:O ratio 1.0 does not obey this trend, showing a smaller than expected surface area, which may explain why sMAO(1.0/80,28/100,14) does not immobilize *rac*-(EBI)$ZrCl_2$.

Step 2: Temperature (T_2)

In the reaction sequence proposed (Scheme 4) step 2 involves the thermal conversion of an aluminoxane precursor species to MAO, *via* an Al–C/Al–O bond metathesis reaction. Therefore the effect of the temperature of this step was investigated.

The temperature of step 2 of the sMAO synthesis (T_2) was varied in 10 °C increments between 70 and 100 °C and the results are collated in Table S3. These data show that an optimized temperature for step 2 is required in order to produce the most active catalyst support for *rac*-(EBI)$ZrCl_2$. The BET surface area generally increases with T_2, however, at 100 °C the surface area is too high (624.1 m^2g^{-1}) and the small pore diameter means the transition metal complex is not uniformly supported. From the perspective of polymerization activity, T_2 = 80 °C produces the optimum sMAO support, so this temperature was used in subsequent studies.

Step 3: Time (t_3)

It is postulated that reaction step 3 (Scheme 4) involves a self-association reaction of the soluble MAO to form sMAO, which precipitates from solution. In their 2003 patent Kaji *et al.* reported that an increased heating time at 100 °C leads to an increase in precipitation rate of sMAO particles.[19] The heating time of step 3 of the sMAO synthesis (t_3) was varied in 4 h increments from 6 to 14 h and the results are displayed in Table S3. Comparison of sMAO(1.2/80,28/100,6) and sMAO-(1.2/80,28/100,14) shows the expected increase in yield with t_3, together with a larger TMA content and higher polymerization activity.

Step 2 and Step 3 conditions combined

It was proposed that integrating two steps of the sMAO synthesis would simplify the procedure and, if it could also produce catalyst supports with relatively high activity, and so reduce the cost of a large-scale process. Hence, after completion of step 1, the reaction mixture was heated to a single temperature ($T_{2,3}$ in °C) for a single time period ($t_{2,3}$ in h), followed by work-up by addition of hexane and isolation of the sMAO precipitate by filtration. The temperature was varied in 10 °C increments from 70 to 100 °C and heating time period was 20 h or 42 h (a combination of the optimum time period of step 2 and 3). The results (Table S4) show that no sMAO was produced at 70 or 80 °C for 20 or 42 h, and instead a colorless solution was obtained. It is postulated that the activation energy for Al–C/Al–O bond metathesis is inaccessible at these temperatures, or that significantly longer reaction times would are required.

The "threshold" temperature for precipitation after 42 h was 90 °C, which produced a good yield (79%) of sMAO, but ultimately a poor catalytic performance with *rac*-(EBI)$ZrCl_2$. Heating to 100 °C for 20 and 42 h periods also produced a good yield of support with disappointing catalytic performance. Similarly, Kaji *et al.* reported in their 2003 patent that when the starting materials were heated directly to 100 °C a composition with non-uniform particle diameter was obtained.[19] These researchers suggested a fully-formed MAO solution is required prior to the self-association reaction to form a sMAO in which the particles have a uniform diameter.

The polymerization data in Table 2 show that sMAO is an effective activator and support for various zirconocene pre-catalysts.

Table 2. Summary of slurry phase polymerization of ethylene using various olefin pre-catalysts based on sMAO.

Complex	[Al]/[Zr]	Activity[a]	Ref
rac-(EBI)$ZrCl_2$	200	13066	This work
($^{n\mathrm{Bu}}$Cp)$_2ZrCl_2$	200	7584	This work
rac-(EBI*)$ZrCl_2$	200	10012	[26]
rac-(SBI*)$ZrCl_2$	300	1740	[26]
rac-(Ind$^{\#}$)$_2ZrCl_2$	300	5971	[26]
Pn*ZrCpCl	200	4209	[25]
Pn*ZrCp$^{\mathrm{Me3}}$Cl	200	4096	[25]

(Ind$^{\#}$) = hexamethylindenyl, Cp$^{\mathrm{Me3}}$ = trimethylcyclopentadienyl, Pn* = permethylpentalene (C_8Me_6); [a] $kg_{PE}mol_{Zr}^{-1}h^{-1}$

CONCLUSIONS

In this report we have developed an optimized laboratory-scale synthesis for solid polymethylaluminoxane (sMAO). This amorphous solid has been extensively characterized using solution and solid-state NMR spectroscopy, which are consistent with a structure featuring long-chain aluminoxane oligomers, with incorporation of "free" TMA and benzoate groups in ca. 14 and 1 mol% respectively, relative to the total CH_3 amount. X-ray pair distribution function (PDF) measurements on sMAO allow comparisons to be made with calculated data for DFT optimized structures of 36 organoaluminum species. The PDF data herein are not of sufficient resolution to pinpoint the exact structure of sMAO, but we postulate that TMA-capped nanotubes (AlOMe)$_{9,t}$·(AlMe$_3$)$_3$ or cage structures (AlO-

$Me)_{20,c},\cdot(AlMe_3)_m$, n>20, m = 1,2, best account for the experimental data. However, further work is required to refine this assumption, and is the focus of our current efforts. SEM imaging and BET physisorption provide insight into the surface structure and porosity of sMAO. sMAO is shown to be a very promising bifunctional support and activator for single site metallocene-based pre-catalysts in slurry-phase ethylene polymerization reactions and we are currently exploring the scope of this material with a range of other transition metal pre-catalysts.

ASSOCIATED CONTENT

Supporting Information.

The Supporting Information is available free of charge on the ACS Publications website at DOI: 10.1021.acs.chemmater.xxxx

Experimental details (general procedures, syntheses and ethylene polymerization), additional characterizing data (solution and solid state NMR, spectroscopy X-ray PDF, particle size distribution, BET surface area), sMAO synthetic optimization and ethylene polymerization data, SEM images for polyethylene samples (PDF).

AUTHOR INFORMATION

Corresponding Author

* E-mail: dermot.ohare@chem.ox.ac.uk.

Author Contributions

The manuscript was written through contributions of all authors. All authors have given approval to the final version of the manuscript.

Notes

The authors declare no competing financial interests.

ACKNOWLEDGMENT

AFRK and JCB thank SCG Chemicals Co., Ltd for funding. PN thanks The Danish Council for Independent Research (grant DFF - 5051-00060). We thank Dr Y. Wu (University of Oxford) for assistance with the PDF measurements. Mr P. Angpanitcharoen (University of Oxford) for SEM images. Dr A. Virden (Malvern Instruments Ltd.) for laser diffraction measurements. Mr P. Holdship (University of Oxford) for ICP-MS analysis. AFRK also thanks Wadham College Oxford for a RJP Williams Junior Research Fellowship.

ABBREVIATIONS

MAO, methylaluminoxane. BA, benzoic acid. TMA, trimethylaluminum. DIP, diisopropylphenyl.

REFERENCES

(1) Zijlstra, H. S.; Harder, S. Methylalumoxane - History, Production, Properties, and Applications. *Eur. J. Inorg. Chem.* 2014, *2015*, 19–43.

(2) Chen, E. Y.; Marks, T. J. Cocatalysts for Metal-Catalyzed Olefin Polymerization: Activators, Activation Processes, and Structure-Activity Relationships. *Chem. Rev.* 2000, *100*, 1391–1434.

(3) Pédeutour, J.-N.; Radhakrishnan, K.; Cramail, H.; Deffieux, A. Reactivity of Metallocene Catalysts for Olefin Polymerization: Influence of Activator Nature and Structure. *Macromol. Rapid Commun.* 2001, *22*, 1095–1123.

(4) Bochmann, M. Kinetic and Mechanistic Aspects of Metallocene Polymerisation Catalysts. *J. Organomet. Chem.* 2004, *689*, 3982–3998.

(5) Zurek, E.; Ziegler, T. Theoretical Studies of the Structure and Function of MAO (Methylaluminoxane). *Prog. Polym. Sci.* 2004, *29*, 107–148.

(6) Negureanu, L.; Hall, R. W.; Butler, L. G.; Simeral, L. A. Methyaluminoxane (MAO) Polymerization Mechanism and Kinetic Model From Ab Initio Molecular Dynamics and Electronic Structure Calculations. *J. Am. Chem. Soc.* 2006, *128*, 16816–16826.

(7) Linnolahti, M.; Severn, J. R.; Pakkanen, T. A. Formation of Nanotubular Methylaluminoxanes and the Nature of the Active Species in Single□Site α□Olefin Polymerization Cataly-

sis. *Angew. Chem. Int. Ed. Engl.* 2008, *47*, 9279–9283.

(8) Glaser, R.; Sun, X. Thermochemistry of the Initial Steps of Methylaluminoxane Formation. Aluminoxanes and Cycloaluminoxanes by Methane Elimination From Dimethylaluminum Hydroxide and Its Dimeric Aggregates. *J. Am. Chem. Soc.* 2011, *133*, 13323–13336.

(9) Linnolahti, M.; Laine, A.; Pakkanen, T. A. Screening the Thermodynamics of Trimethylaluminum-Hydrolysis Products and Their Co-Catalytic Performance in Olefin-Polymerization Catalysis. *Chem.–Eur. J.* 2013, *19*, 7133–7142.

(10) Ghiotto, F.; Pateraki, C.; Tanskanen, J.; Severn, J. R.; Luehmann, N.; Kusmin, A.; Stellbrink, J.; Linnolahti, M.; Bochmann, M. Probing the Structure of Methylalumoxane (MAO) by a Combined Chemical, Spectroscopic, Neutron Scattering, and Computational Approach. *Organometallics* 2013, *32*, 3354–3362.

(11) Hirvi, J. T.; Bochmann, M.; Severn, J. R.; Linnolahti, M. Formation of Octameric Methylaluminoxanes by Hydrolysis of Trimethylaluminum and the Mechanisms of Catalyst Activation in Single-Site α-Olefin Polymerization Catalysis. *ChemPhysChem* 2014, *15*, 2732–2742.

(12) Kuklin, M. S.; Hirvi, J. T.; Bochmann, M.; Linnolahti, M. Toward Controlling the Metallocene/Methylaluminoxane-Catalyzed Olefin Polymerization Process by a Computational Approach. *Organometallics* 2015, *34*, 3586–3597.

(13) Malpass, D. B.; Monfiston, D. J.; Palmaka, S. W.; Rogers, J. S.; Smith, G. M. Polyalkylaluminoxane Compositions Formed by Non-Hydrolytic Means. US Pat. US 5777143 1997.

(14) Meisters, A.; Mole, T. Exhaustive C-Methylation of Carboxylic Acids by Trimethylaluminium: a New Route to *t*-Butyl Compounds. *Aust. J. Chem.* 1974, *27*, 1665–1672.

(15) Cramail, H.; Radhakrishnan, K.; Deffieux, A. New Synthetic Route to Methylaluminoxane for Ethylene Polymerisation in the Presence of Zirconocene. *C. R. Chim.* 2002, *5*, 49–52.

(16) Radhakrishnan, K.; Cramail, H.; Deffieux, A.; François, P.; Momtaz, A. Ethylene Polymerization Studies with an MAO Synthesized by a Non-Hydrolytic Synthetic Route. *Macromol. Rapid Commun.* 2002, *23*, 829–833.

(17) Dalet, T.; Cramail, H.; Deffieux, A. Non-Hydrolytic Route to Aluminoxane-Type Derivative for Metallocene Activation Towards Olefin Polymerisation. *Macromol. Chem. Phys.* 2004, *205*, 1394–1401.

(18) Tudella, J.; Ribeiro, M. R.; Cramail, H.; Deffieux, A. Novel Organic Activators for Single Site Iron Catalysts. *Macromol. Chem. Phys.* 2007, *208*, 815–822.

(19) Kaji, E.; Yoshioka, E. Solid Polymethylaluminoxane Composition and Method for Manufacturing Same. US Patent. 8,404,880 B2 2013.

(20) Wright, C. M. R.; Turner, Z. R.; Buffet, J.-C.; O Hare, D. Tungsten Imido Catalysts for Selective Ethylene Dimerisation. *Chem. Commun.* 2016, *52*, 2850–2853.

(21) Buffet, J.-C.; Turner, Z. R.; Cooper, R. T.; O'Hare, D. Ethylene Polymerisation Using Solid Catalysts Based on Layered Double Hydroxides. *Polym. Chem.* 2015, *6*, 2493–2503.

(22) Buffet, J.-C.; Wanna, N.; Arnold, T. A. Q.; Gibson, E. K.; Wells, P. P.; Wang, Q.; Tantirungrotechai, J.; O'Hare, D. Highly Tunable Catalyst Supports for Single-Site Ethylene Polymerization. *Chem. Mater.* 2015, *27*, 1495–1501.

(23) Buffet, J.-C.; Arnold, T. A. Q.; Turner, Z. R.; Angpanitcharoen, P.; O'Hare, D. Synthesis and Characterisation of Permethylindenyl Zirconium Complexes and Their Use in Ethylene Polymerisation. *RSC Adv.* 2015, *5*, 87456–87464.

(24) Buffet, J.-C.; Byles, C. F. H.; Felton, R.; Chen, C.; O Hare, D. Metallocene Supported Core@LDH Catalysts for Slurry Phase Ethylene Polymerisation. *Chem. Commun.* 2016, *52*, 4076–4079.

(25) Fraser, D. A. X.; Turner, Z. R.; Buffet, J.-C.; O'Hare, D. Titanium and Zirconium Permethylpentalene Complexes, Pn*MCp^{R}X, as Ethylene Polymerization Catalysts. *Organometallics* 2016, *35*, 2664–2674.

(26) Arnold, T. A. Q.; Turner, Z. R.; Buffet, J.-C.; O'Hare, D. Polymethylaluminoxane Supported Zirconocene Catalysts for Polymerisation of Ethylene. *J. Organomet. Chem.* 2016, *822*, 85–90.

(27) Severn, J. R.; Chadwick, J. C.; Duchateau, R.; Friederichs, N. "Bound but Not Gagged" Immobilizing Single-Site α-Olefin Polymerization Catalysts. *Chem. Rev.* 2005, *105*, 4073–4147.

(28) Sinn, H. Proposals for Structure and Effect of Methylalumoxane Based on Mass Balances and Phase Separation Experiments. *Macromol. Symp.* 2011, *97*, 27–52.

(29) Bryant, P. L.; Harwell, C. R.; Mrse, A. A.; Emery, E. F.; Gan, Z.; Caldwell, T.; Reyes, A. P.; Kuhns, P.; Hoyt, D. W.; Simeral, L. S.; Hall, R. W.; Butler, L. G. Structural Characterization of MAO and Related Aluminum Complexes. 1. Solid-State ^{27}Al NMR with Comparison to EFG Tensors From Ab Initio Molecular

Orbital Calculations. *J. Am. Chem. Soc.* 2001, *123*, 12009–12017.

(30) Janiak, C.; Rieger, B.; Voelkel, R.; Braun, H.-G. Polymeric Aluminoxanes: a Possible Cocatalytic Support Material for Ziegler–Natta-Type Metallocene Catalysts. *J. Polym. Sci. A Polym. Chem.* 1993, *31*, 2959–2968.

(31) Falls, Z.; Zurek, E.; Autschbach, J. Computational Prediction and Analysis of the ^{27}Al Solid-State NMR Spectrum of Methylaluminoxane (MAO) at Variable Temperatures and Field Strengths. *Phys. Chem. Chem. Phys.* 2016, *18*, 24106–24118.

(32) Soper, A. K.; Barney, E. R. Extracting the Pair Distribution Function From White-Beam X-Ray Total Scattering Data. *J. Appl. Crystallogr.* 2011, *44*, 714–726.

(33) Farrow, C. L.; Juhás, P.; Liu, J. W.; Bryndin, D.; Božin, E. S.; Bloch, J.; Proffen, T.; Billinge, S. J. L. PDFfit2 and PDFgui: Computer Programs for Studying Nanostructure in Crystals. *J. Phys.: Condens. Matter.* 2007, *19*, 335219.

(34) Linnolahti, M.; Severn, J. R.; Pakkanen, T. A. Are Aluminoxanes Nanotubular? Structural Evidence From a Quantum Chemical Study. *Angew. Chem. Int. Ed. Engl.* 2006, *45*, 3331–3334.

(35) Boudene, Z.; de Bruin, T.; Toulhoat, H.; Raybaud, P. A QSPR Investigation of Thermal Stability of $[Al(CH_3)O]_n$ Oligomers in Methylaluminoxane Solution: the Identification of a Geometry-Based Descriptor. *Organometallics* 2012, *31*, 8312–8322.

(36) Falls, Z.; Tymińska, N.; Zurek, E. The Dynamic Equilibrium Between $(AlOMe)_n$ Cages and $(AlOMe)_n{\cdot}(AlMe_3)_m$ Nanotubes in Methylaluminoxane (MAO): a First-Principles Investigation. *Macromolecules* 2014, *47*, 8556–8569.

(37) Thommes, M.; Kaneko, K.; Neimark, A. V.; Olivier, J. P.; Rodriguez-Reinoso, F.; Rouquerol, J.; Sing, K. S. W. Physisorption of Gases, with Special Reference to the Evaluation of Surface Area and Pore Size Distribution (IUPAC Technical Report). *Pure Appl. Chem.* 2015, *87*, 1051–1069.

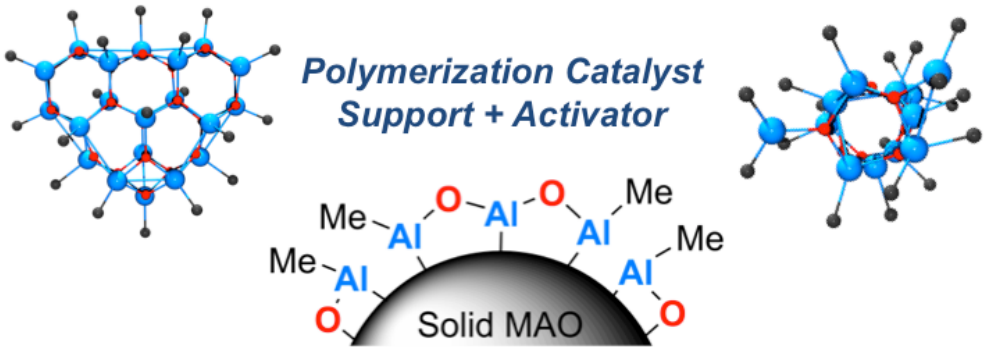
Polymerization Catalyst
Support + Activator
Me
Al
O
Al
O
Al
Me
Me
Al
Al
Me
O
O
Solid MAO